Nucleonic Binding States in Nonspherical Nuclei: Asymptotic Representation

A. J. RASSEY
Department of Physics, University of California, Los Angeles, California
(Received February 12, 1957)

An alternative description is given for Nilsson's analysis of nucleonic motion in a strongly deformed nuclear field. The aim is to obtain the single-particle states for the region of strong deformation in terms of a representation which is especially suited for that region in contrast to the spherical representation used by Nilsson.

The eigenvectors of a 3-dimensional *anisotropic* harmonic oscillator (H.O.) are used as a basic set to calculate the single-particle wave functions and energy eigenvalues. Two immediate advantages of choosing this basic set are: first, the matrix elements between single-particle states are expressible in terms of the rather simple analytic expressions obtained for these matrix elements in the H.O. representation and second, the expansion of the particle wave functions generally is rather pure, so that in many instances the leading term in the expansion is sufficient for calculations. Thus, good approximate calculations are easily obtainable. The high degree of purity of state has been taken advantage of previously by several authors to classify states in the strong-deformation region using the "almost good" quantum numbers of the basic set (asymptotic quantum numbers).

Separate level spectra are given for protons and neutrons similar to the Mottleson and Nilsson scheme but more extensive (including some $N=7$ shell neutron levels). A large gap at neutron number 152 offers a partial explanation of the closing of a subshell there previously interpreted by Ghiorso *et al.* from α-decay curves.

New approximate transition selection rules are given for allowed and first-forbidden β decay. For allowed transitions the relative speed varies approximately as $10^{-|\Delta N_z|}$. For first forbidden transitions, relative speeds are tabulated as functions of ΔN_r. The latter transitions are generally cut down by a factor $(10^{-5}-10^{-3})$ for $|\Delta N_r| \geq 2$.

I. INTRODUCTION

RECENT advancements have been made in accounting for nuclear properties in the region between closed shells. In this region it is found that the isotropic-field description afforded by the shell model is inadequate by itself to account for many of the observed nuclear properties. In particular, nuclei in the region far from closed shells have been found to possess large quadrupole moments which imply proton charge distributions which are very different from spherical symmetry. That is to say, the nuclear field is anisotropic.

As a result of nucleonic motion in this deformed field, the angular momentum of the nucleons is no longer constant and, thus, the nucleus must possess some other angular momentum such that a conserved total angular momentum is insured. This additional angular momentum is attributed to the rotation of the nucleons as an aggregate (collective rotation). In addition, a new variable must also be introduced to account for the nuclear shape, i.e., oscillations of the nuclear shape about some equilibrium position (collective oscillations). In general, then, account should be taken of the collective modes of motion, the intrinsic motion of the individual nucleons, and any interplay between the collective types and intrinsic motions.[1]

However, if we restrict ourselves to the region far from closed shells, it is possible to make an approximate separation between the collective modes of motion and the intrinsic nucleonic motion relative to the deformed but fixed nuclear field. The nuclear wave function can then be written as a product of functions each of which represents one mode of the motion, i.e., rotational, vibrational, and intrinsic.[1–3] It is this region that is of interest here. In particular, we shall be interested in obtaining a description of the intrinsic motion of individual nucleons in the deformed nuclear potential.

Recently such a description has been given by Nilsson,[4,5] who has calculated the level spectrum of the intrinsic motion of individual nucleons assuming single-particle motion in a spheroidal harmonic oscillator (H.O.) potential well with strong spin-orbit and $\mathbf{l}^2$ coupling. The spheroidal H.O. potential is split into a spherically symmetric term and a term giving the coupling of the particle to the nuclear symmetry axis as a function of the deformation. Retaining all but the spherically symmetric term of the H.O. as perturbations, Nilsson uses the eigenvectors of the 3-dimensional *isotropic* H.O. as a basic set. Basically then, Nilsson begins with a spherical nucleus and proceeds via the coupling energies to generate a deformed field.

As a consequence of Nilsson's model, with sufficiently large deformation there is an approximate separation of the nucleonic motion into oscillations along the nuclear symmetry axis and oscillations in a plane normal to this axis. In this limit an alternative representation for obtaining the single-particle wave functions immediately suggests itself,[6] namely, to expand the nucleon wave function in terms of the eigenvectors of an *anisotropic* H.O. potential. By doing this, one obtains a

[1] A. Bohr, Kgl. Danske Videnskab. Selskab, Mat.-fys. Medd. **26**, No. 14 (1952).

[2] This limiting case is called the strong-coupling scheme after Bohr.

[3] For the appropriately symmetrized nuclear wave function see A. Bohr and B. R. Mottelson, [Kgl. Danske Videnskab. Selskab, Mat.-fys. Medd. **27**, No. 16 (1953)].

[4] S. G. Nilsson, Kgl. Danske Videnskab. Selskab, Mat.-fys. Medd. **29**, No. 16 (1955).

[5] For a list of other authors who have considered the motion of nucleons in a deformed potential, see Nilsson, (reference 4, p. 8); also, more recently, K. Gottfried, [Phys. Rev. **103**, 1017 (1956)].

[6] Suggested by Nilsson, reference 4, Appendix B.

description of the motion which conforms more closely to the motion assumed by the particle in the strongly deformed field. Formally, we may say that in the region of very strong deformations the nucleonic wave functions are more nearly pure states when expanded in terms of the eigenvectors which we propose. In this paper we shall obtain the solutions of this alternative approach and examine some of the resulting implications.

We restrict ourselves to dealing with the intrinsic motion of the nucleons in a deformed static nuclear field neglecting, as mentioned above, the collective modes of motion and any interplay between the collective and intrinsic motion. In fact, we shall consider independent-particle motion under the influence of the collective distorted field only. For more of the physical content underlying the proposed interaction, we refer the reader to Nilsson's paper and references contained therein.

The particle motion in the deformed nuclear field will be governed by a single-particle Hamiltonian consisting of a cylindrically symmetric H.O. potential with appropriate spin-orbit and $\mathbf{l}^2$ coupling. With a Hamiltonian of this type, the only constants of the motion are the component of the total angular momentum along the symmetry axis with quantum number Ω and the parity.

In Sec. II we obtain the single-particle eigenvalues and eigenvectors by using an electronic digital computer. The results are arranged in convenient tabular form (Table I).

In Sec. III a few limited applications of these results are given. In particular, some new transition selection rules are found and separate level spectra for protons and neutrons are presented.

II. CALCULATION OF LEVEL SPECTRUM

A. Method of Solution

In this section we present an outline of the calculations performed and discuss some of the results obtained. The first calculation consists of finding the eigenvectors of a cylindrically symmetric H.O. These eigenvectors are then used as a basic set for the expansion of the nucleon wave functions of the total Hamiltonian. Next we impose the condition of volume preservation and pass to the limit required for very strong deformation. The coupling energies are then found between states of the basic set and are grouped along with the diagonal energy terms of the H.O. to form submatrices of the total energy. These submatrices are labeled by the quantum number Ω and, further, are diagonalized exactly, yielding the eigenvalues and eigenvectors of the substates corresponding to a given Ω.

Let us now consider the calculation in more detail. The approximate separation of the nucleon motion in the manner described above can be accounted for by a single-particle Hamiltonian of the following type [see Nilsson discussion of Eq. (2)]:

$$H=H_0+C\mathbf{l}\cdot\mathbf{s}+D\mathbf{l}^2, \tag{1a}$$

where

$$H_0=-(\hbar^2/2m)\nabla'^2+\tfrac{1}{2}m(\omega_r^2r'^2+\omega_z^2z'^2), \tag{1b}$$

r' and z' being the coordinates of the particle in a coordinate system fixed in the nucleus. H_0 and the spin-orbit term follow from the usual formulation of the shell-model Hamiltonian. To complete the interaction Nilsson has added an $\mathbf{l}^2$ coupling term. The level sequence generated by deforming the oscillator potential in this fashion lies somewhere in between that obtained from the H.O. and that obtained from the square well potential. The choice of $\mathbf{l}\cdot\mathbf{s}$, and $\mathbf{l}^2$ coupling strengths has been considered previously by Nilsson, who has selected them to reproduce the single-particle level scheme of the shell model for the spherical case of (1a) and (1b). For simplicity, we denote $C\mathbf{l}\cdot\mathbf{s}+D\mathbf{l}^2$ by H' which will be regarded as a perturbative term.

As seen from (1b), in the energy representation, the operators commuting with H_0 are $\mathbf{l}_z$ and $\mathbf{s}_z$ with quantum numbers Λ and Σ, respectively. The remaining quantum numbers N_r and N_z together with Λ and Σ define the following aspects of the particle motion: N_z and N_r give the number of oscillator quanta along the symmetry axis and in a plane perpendicular to the symmetry axis respectively, while Λ and Σ are the components of the particle orbital and spin angular momentum along the symmetry axis, respectively. It is also convenient to define the total number of oscillator quanta N given by $N=N_r+N_z$. It should be pointed out that these quantum numbers have been used extensively already by other authors to characterize the strong-deformation states. They have previously been called the asymptotic quantum numbers.

As seen from (1a), none of the above operators commute with the total Hamiltonian. Instead, the only constants of the motion are given by $\mathbf{j}_z=\mathbf{l}_z+\mathbf{s}_z$ (the projection of the total angular momentum on the symmetry axis) with quantum number Ω, and the parity. The states characterized by a given Ω will be given as linear combinations of the base vectors $\psi(NN_z\Lambda\Sigma)$, where $\Omega=\Lambda+\Sigma$, while the parity of each state is even or odd according to even or odd N. These states are doubly degenerate corresponding to $\pm\Omega$.

To put the results in dimensionless form we introduce the following independent variables $\rho=(m\omega_r/\hbar)^{\frac{1}{2}}r'$, etc. Expressing ∇^2 in cylindrical coordinates, (1b) is separable in ρ, ϕ, and z, where ϕ as usual, is the angle of rotation in the ρ plane. The solution of

$$H_0\psi(NN_z\Lambda\Sigma)=E_{NN_z}\psi(NN_z\Lambda\Sigma) \tag{2}$$

are obtained as

$$E_{NN_z}=\hbar\omega_r(N-N_z+1)+\hbar\omega_z(N_z+\tfrac{1}{2}), \tag{3}$$

with $\psi(NN_z\Lambda\Sigma)$ given as a product of $R\Phi Z$, the three

factors being specified as follows:

$$R_{N_r\Lambda}\sim\exp(-\tfrac{1}{2}\rho^2)\rho^{|\Lambda|}\mathfrak{R}_{N_r\Lambda}(\rho),$$

where

$$\mathfrak{R}_{N_r\Lambda}(\rho)=1+\frac{(|\Lambda|-N_r)\rho^2}{2(1+|\Lambda|)}+\frac{(|\Lambda|-N_r)(|\Lambda|-N_r+2)\rho^4}{2\times4(1+|\Lambda|)(2+|\Lambda|)}+\cdots,$$

$$\Phi_\Lambda\sim e^{i\Lambda\phi},$$

where, as usual, Λ only takes on integral values; finally,

$$Z_{N_z}\sim\exp(-\tfrac{1}{2}z^2)h_{N_z}(z),$$

where $h_{N_z}(z)$ are the well-known Hermite polynomials.[7]

We now wish to have the solutions appropriate to very strongly deformed nuclei. To determine these solutions, we begin by imposing the condition of volume preservation which yields

$$\omega_r^2\omega_z=\omega_0^3=\text{constant}. \tag{4}$$

Next to introduce the deformation parameter ϵ defined in the following manner:

$$\omega_r=\omega_0e^{\epsilon/3},\quad \omega_z=\omega_0e^{-2\epsilon/3}. \tag{5}$$

It is readily seen that these expressions satisfy Eq. (4). To second order in ϵ, Eqs. (5) expand to

$$\omega_r=\omega_0(1+\tfrac{1}{3}\epsilon+\tfrac{1}{18}\epsilon^2),\quad \omega_z=\omega_0(1-\tfrac{2}{3}\epsilon+\tfrac{2}{9}\epsilon^2). \tag{5'}$$

The slight difference between ϵ and Nilsson's deformation parameter δ occurs because of the slightly different manner in which the volume preservation condition is imposed. In Nilsson's paper, constant volume is assured only to first order distortions; here the volume is preserved to all orders [see Nilsson (3a) and (3b)]. Hence, to first order, ϵ and δ are equal.

In the limit of small ϵ, then, the energy is given by

$$E_{NN_z}=\hbar\omega_0[(1+\tfrac{1}{9}\epsilon^2)(N+\tfrac{3}{2})-\tfrac{1}{3}(3N_z-N)\epsilon], \tag{6}$$

where we have neglected a term $(3N_z-N)\epsilon^2/18$ which is of the order of $\frac{1}{15}$ to $\frac{1}{20}$ of the $\frac{1}{3}\epsilon$ term when ϵ takes on the values 0.2 and 0.3, respectively. It should be pointed out, however, that Eq. (6) as written is rigorously true to order ϵ^2 when summing the energy E_{NN_z} over closed shells since $\sum(3N_z-N)$ vanishes identically. In any event, in most cases the energy levels will be changed only slightly, while the wave functions not at all if the term were included (small perturbation effect). We prefer not to include these second order effects at this time in order to duplicate Nilsson's results.

In this representation it turns out that such quantities as $x^\pm=x\pm iy$, $l^\pm=l_x\pm il_y$, z, l_z, $\mathbf{l}^2$, and $\mathbf{l}\cdot\mathbf{s}$ can be written in rather simple analytic form. These are

$$\langle N_r-1\ \Lambda\pm1|x^\pm|N_r\Lambda\rangle=\mp[\tfrac{1}{2}(N_r\mp\Lambda)]^{\frac{1}{2}},$$
$$\langle N_r+1\ \Lambda\pm1|x^\pm|N_r\Lambda\rangle=-\pm[\tfrac{1}{2}(N_r\pm\Lambda+2)]^{\frac{1}{2}}, \tag{7a}$$

$$\langle N_{z'}|z|N_z\rangle=(\tfrac{1}{2}N_{z\text{ upper}})^{\frac{1}{2}}, \tag{7b}$$

where $N_{z\text{ upper}}$ denotes the larger of the two N_z values;

$$\langle N_z+1\ \Lambda\pm1|l^\pm|N_z\Lambda\rangle=[(N_r\mp\Lambda)(N_z+1)]^{\frac{1}{2}}, \tag{7c}$$

$$\langle N_z-1\ \Lambda\pm1|l^\pm|N_z\Lambda\rangle=[(N_r\pm\Lambda+2)N_z]^{\frac{1}{2}}, \tag{7d}$$

$$\langle NN_z\Lambda|l_z|NN_z\Lambda\rangle=\Lambda, \tag{7e}$$

$$\langle N_z+2\ \Lambda|\mathbf{l}^2|N_z\Lambda\rangle=[(N_r-\Lambda)(N_r+\Lambda)\times(N_z+1)(N_z+2)]^{\frac{1}{2}}, \tag{7f}$$

$$\langle N_z-2\ \Lambda|\mathbf{l}^2|N_z\Lambda\rangle=[(N_r+\Lambda+2)\times(N_r-\Lambda+2)N_z(N_z-1)]^{\frac{1}{2}}, \tag{7g}$$

$$\mathbf{l}^2{}_{\text{diagonal}}=\Lambda^2+2N_zN_r+2N_z+N_r, \tag{7h}$$

$$\mathbf{l}\cdot\mathbf{s}_{\text{diagonal}}=\Lambda\Sigma, \tag{7i}$$

$$\langle N_z+1\ \Lambda\pm1\ \Sigma'|\mathbf{l}\cdot\mathbf{s}|N_z\Lambda\Sigma\rangle=\tfrac{1}{2}l^\pm{}_{\text{off diagonal}}, \tag{7j}$$

$$\langle N_z-1\ \Lambda\pm1\ \Sigma'|\mathbf{l}\cdot\mathbf{s}|N_z\Lambda\Sigma\rangle=\tfrac{1}{2}l^\pm{}_{\text{off diagonal}}. \tag{7k}$$

It should be mentioned that to first order in ϵ, matrix elements of $\mathbf{l}^2$ vanish except those in the same major shell.

The appropriate selection rules are tabulated for convenience (Table I).

Additional selection rules have been tabulated by Alaga,[8] in particular those for allowed and first-forbidden β transitions.

Turning now to the solutions of (1a), the energy eigenvalues of the total H are given by

$$E_{NN_z\Omega}=\hbar\omega_0[(N+\tfrac{3}{2})(1+\tfrac{1}{9}\epsilon^2)+r(N,N_z,\Omega)]. \tag{8}$$

As written, the equation indicates that a state is characterized by N, N_z, and Ω. Rigorously this cannot be so, since N_z is no longer a good quantum number when considering the total H. However, upon obtaining the eigenvectors, $\chi_\Omega{}^N$, corresponding to each eigenvalue r, it is immediately apparent that in the expansion of $\chi_\Omega{}^N=\sum A_{NN_z}\psi(NN_z\Omega)$ one coefficient A_{NN_z} is

TABLE I. Selection rules for a cylindrically symmetric harmonic oscillator.

Operator	Selection rule	
$\mathbf{1}$	$\Delta N=0$, $\Delta N_z=0$, $\Delta\Lambda=0$, $\Delta\Omega=0$	No
$\mathbf{x}^\pm$	$\Delta N=\pm1$, $\Delta N_z=0$, $\Delta\Lambda=\pm1$, $\Delta\Omega=\pm1$	Yes
$\mathbf{z}$	$\Delta N=\pm1$, $\Delta N_z=\pm1$, $\Delta\Lambda=0$, $\Delta\Omega=0$	Yes
$\mathbf{l}^\pm$	$\Delta N=0$, $\Delta N_z=\pm1$, $\Delta\Lambda=\pm1$, $\Delta\Omega=\pm1$	No
	$\Delta N=\pm2$, $\Delta N_z=\pm1$, $\Delta\Lambda=\pm1$, $\Delta\Omega=\pm1$	No
$\mathbf{l}_z$	$\Delta N=0$, $\Delta N_z=0$, $\Delta\Lambda=0$, $\Delta\Omega=0$	No
$\boldsymbol{\sigma}$	$\Delta N=0$, $\Delta N_z=0$, $\Delta\Lambda=0$, $\Delta\Omega=0,\pm1$	No
$\mathbf{l}\cdot\boldsymbol{\sigma}$	$\Delta N=0$, $\Delta N_z=0,\pm1$; $\Delta\Lambda=0,\pm1$; $\Delta\Omega=0$,	No
$\mathbf{l}^2$	$\Delta N=0$, $\Delta N_z=0,\pm2$; $\Delta\Lambda=0$, $\Delta\Omega=0$	No

[7] Solutions of Eq. (1b) are worked out in detail in L. Pauling and E. B. Wilson, *Introduction to Quantum Mechanics* (McGraw-Hill Book Company, Inc., New York, 1935), p. 105.

[8] G. Alaga, Phys. Rev. **100**, 432 (1955).

TABLE II. Eigenfunctions for the deformed field: asymptotic representation. ψ indicates the base vector $|NN_z\Lambda\Sigma\rangle$. Where the dominant ψ in a set is not clearly indicated as given in Sec. II, Part B, they have been labelled with an asterisk. The numbers adjacent to the $|NN_z\Lambda\Sigma\rangle$ are the orbit numbers prescribed by Nilsson.[a]

N	Ω	ψ		$\epsilon=0.2$	$\epsilon=0.3$
4	$9/2$	$404\uparrow$	18	1.000	1.000
4	$7/2$	$404\downarrow$	25	0.972	0.979
				−0.235	−0.204
				0.235	0.204
		$413\uparrow$	21	0.977	0.979
4	$5/2$	$402\uparrow$	31	0.973	0.983
				−0.201	−0.155
				−0.111	−0.096
				0.146	0.117
		$413\downarrow$	27	0.915	0.941
				−0.376	−0.317
				0.177	0.140
				0.349	0.301
		$422\uparrow$	22	0.920	0.944
4	$3/2$	$402\downarrow$	42	0.960	0.973
				−0.234	−0.199
				−0.140	−0.110
				0.062	0.041
				0.179	0.166
		$411\uparrow$	33	0.902	0.936
				−0.359	−0.274
				−0.160	−0.146
				0.199	0.150
				0.189	0.162
		$422\downarrow$	29	0.806	0.874
				−0.525	−0.433
				0.084	0.055
				0.311	0.241
				0.449	0.386
		$431\uparrow$	23	0.834	0.889
4	$1/2$	$400\uparrow$	51	0.960	0.974
				−0.227	−0.186
				−0.150	−0.121
				0.063	0.038
				0.016	0.010
				0.160	0.143
		$411\downarrow$	43	0.878	0.922
				−0.374	−0.309
				−0.211	−0.166
				0.138	0.078
				0.205	0.163
				0.192	0.201
		$420\uparrow$	34	0.783	0.860
				−0.535	−0.412
				−0.149	−0.153
				0.075	0.047
				0.319	0.243
				0.180	0.195
		$431\downarrow$	30	0.603	0.757
				−0.704	−0.572
				0.069	0.038
				0.199	0.125
				0.438	0.335
				0.549	0.477
		$440\uparrow$	24	0.680	0.802
5	$11/2$	$505\uparrow$	28	1.000	1.000
5	$9/2$	$505\downarrow$	40	0.975	0.980
				−0.242	−0.200
				0.242	0.200
		$514\uparrow$	32	0.975	0.980
5	$7/2$	$503\uparrow$	48	0.975	0.984
				−0.192	−0.147
				−0.115	−0.102
				0.140	0.110
		$514\downarrow$	41	0.924	0.945
				−0.355	−0.302
				0.175	0.142
				0.330	0.291
		$523\uparrow$	35	0.928	0.946
5	$5/2$	$503\downarrow$	61	0.961	0.972
				−0.225	−0.196
				−0.148	−0.118
				0.066	0.044
				0.172	0.165
		$512\uparrow$	50	0.908	0.938
				−0.342	−0.260
				−0.173	−0.161
				0.204	0.156
				0.181	0.146
		$523\downarrow$	44	0.829	0.885
				−0.488	−0.414
				0.077	0.054
				0.305	0.246
				0.416	0.369
		$532\uparrow$	36	0.853	0.895
5	$3/2$	$501\uparrow$	70	0.960	0.974
				−0.216	−0.177
				−0.163	−0.135
				0.063	0.040
				0.021	0.014
				0.150	0.131
		$512\downarrow$	62	0.878	0.919
				−0.357	−0.306
				−0.240	−0.191
				0.148	0.093
				0.213	0.175
				0.180	0.200
		$521\uparrow$	52	0.795	0.862
				−0.505	−0.388
				−0.184	−0.192
				0.078	0.047
				0.347	0.265
				0.177	0.163
		$532\downarrow$	46	0.666	0.785
				−0.632	−0.534
				0.063	0.039
				0.172	0.118
				0.426	0.345
				0.490	0.443
		$541\uparrow$	37	0.738	0.818

[a] See reference 4.

TABLE II.—*Continued.*

N	Ω	ψ		$\epsilon=0.2$	$\epsilon=0.3$
5	$\frac{1}{2}$	501↓	A	0.955	0.970
				−0.224	−0.190
				−0.177	−0.142
				0.078	0.050
				0.027	0.017
				−0.017	−0.008
				0.155	0.146
		510↑	71	0.874	0.916
				−0.357	−0.295
				−0.250	−0.207
				0.147	0.089
				0.033	0.023
				0.227	0.181
				0.163	0.166
		521↓	63	0.738	0.834
				−0.476	−0.409
				−0.288	−0.234
				0.260	0.147
				0.062	0.051
				0.333	0.279
				0.105	0.185
		530↑	53	0.647	0.756
				−0.665	−0.533
				−0.116	−0.171
				0.084	0.045
				0.156	0.096
				0.435	0.341
				0.102	0.156
		541↓	47	0.391	0.615
				−0.785	−0.685
				0.045	0.024
				0.156	0.095
				0.311	0.215
				0.526	0.437
				0.547	0.524
		550↑	38	0.549	0.692
6	$1\frac{3}{2}$	606↑	39	1.000	1.000
6	$1\frac{1}{2}$	606↓	56	0.978	0.983
				−0.217	−0.192
				0.217	0.192
		615↑	45	0.978	0.983
6	$\frac{9}{2}$	604↑	66	0.976	0.984
				−0.186	−0.142
				−0.116	−0.105
				0.138	0.105
		615↓	59	0.931	0.949
				−0.337	−0.296
				0.171	0.142
				0.313	0.281
		624↑	49	0.934	0.949
6	$\frac{7}{2}$	604↓		0.962	0.973
				−0.216	−0.192
				−0.152	−0.124
				0.064	0.045
				0.165	0.162
		613↑	67	0.912	0.940
				−0.330	−0.248
				−0.178	−0.170
				0.204	0.159
				0.179	0.137
		624↓	64	0.846	0.894
				−0.459	−0.397
				0.071	0.052
				0.298	0.247
				0.391	0.353
		633↑	54	0.868	0.901
6	$\frac{5}{2}$	602↑		0.961	0.974
				−0.209	−0.171
				−0.169	−0.144
				0.062	0.040
				0.023	0.017
				0.145	0.124
		613↓		0.883	0.919
				−0.341	−0.298
				−0.251	−0.205
				0.144	0.097
				0.215	0.181
				0.170	0.196
		622↑	72	0.806	0.865
				−0.485	−0.368
				−0.200	−0.211
				0.078	0.046
				0.353	0.275
				0.182	0.148
		633↓	65	0.702	0.804
				−0.586	−0.504
				0.059	0.039
				0.154	0.112
				0.415	0.347
				0.453	0.417
		642↑	55	0.771	0.832
6	$\frac{3}{2}$	602↓		0.953	0.968
				−0.217	−0.189
				−0.192	−0.155
				0.082	0.056
				0.034	0.021
				−0.021	−0.010
				0.149	0.145
		611↑		0.876	0.915
				−0.343	−0.284
				−0.266	−0.229
				0.145	0.092
				0.043	0.032
				0.240	0.192
				0.155	0.149
		622↓		0.741	0.828
				−0.446	−0.395
				−0.323	−0.268
				0.258	0.166
				0.057	0.051
				0.341	0.295
				0.090	0.178
		631↑	73	0.666	0.761
				−0.636	−0.502
				−0.158	−0.215
				0.088	0.050
				0.164	0.097
				0.468	0.374
				0.129	0.133
		642↓	68	0.473	0.665
				−0.711	−0.623
				0.037	0.021
				0.140	0.093
				0.264	0.194
				0.513	0.438
				0.496	0.475
		651↑	57	0.633	0.732

TABLE II.—*Continued.*

N	Ω	ψ		$\epsilon=0.2$	$\epsilon=0.3$
6	$\frac{1}{2}$	600↑		0.952	0.968
				−0.215	−0.183
				−0.195	−0.160
				0.081	0.054
				0.037	0.024
				−0.004	−0.002
				−0.021	−0.010
				0.144	0.134
		611↓		0.860	0.906
				−0.341	−0.295
				−0.295	−0.243
				0.173	0.113
				−0.051	−0.023
				0.063	0.039
				0.240	0.197
				0.144	0.162
		620↑		0.734	0.821
				−0.454	−0.391
				−0.324	−0.283
				0.051	0.040
				0.263	0.163
				0.072	0.052
				0.366	0.307
				0.100	0.141
		631↓	B	0.538	0.706
				−0.520	−0.488
				0.418	0.246
				−0.340	−0.293
				0.070	0.050
				0.070	0.089
				0.408	0.375
				−0.082	0.109
		640↑	74	0.523	0.633
				−0.013	−0.156
				−0.737	−0.642
				−0.056	−0.023
				−0.205	−0.111
				−0.253	−0.151
				−0.491	−0.423
				0.009	−0.078
		651↓	69	0.797	0.765
				−0.118	−0.440
				0.033	0.018
				0.109	0.065
				0.257	0.174
				0.404	0.310
				0.565	0.512
				0.429	0.572
		606↑	60	0.504	0.530
7	$\frac{9}{2}$	705↓		0.065	0.050
		714↑		0.291	0.246
		725↓		0.370	0.339
		734↑*		0.880	0.907

N	Ω	ψ	$\epsilon=0.2$	$\epsilon=0.3$
7	$\frac{7}{2}$	703↑	0.054	0.038
		714↓	0.140	0.106
		723↑	0.405	0.345
		734↓	0.426	0.396
		743↑*	0.795	0.844
7	$\frac{5}{2}$	703↓	0.031	0.020
		712↑	0.128	0.090
		723↓	0.234	0.178
		732↑	0.501	0.435
		743↓	0.463	0.444
		752↑*	0.680	0.757
7	$\frac{3}{2}$		0.070	0.053
			0.064	0.087
			0.414	0.392
			0.084	0.099
		741↑*	0.717	0.643
			0.074	−0.608
			−0.542	−0.206
		701↑	−0.055	−0.025
		712↓	−0.202	0.121
		721↑	−0.263	0.155
		732↓	−0.522	0.464
		741↑	−0.228	0.075
		752↓*	0.748	0.509
		761↑	−0.047	−0.693
			0.028	0.016
			0.088	0.055
			0.229	0.163
			0.345	0.272
			0.473	0.509
			0.528	0.481
		761↑*	0.563	0.637
7	$\frac{1}{2}$		−0.010	−0.018
			−0.126	−0.109
			0.011	−0.099
			−0.421	−0.437
			0.317	0.035
		750↑*	0.694	0.717
			−0.118	0.093
			−0.459	−0.512
		701↓	−0.057	−0.018
		710↑	−0.153	−0.067
		721↓	−0.341	−0.209
		730↑	−0.336	−0.209
		741↓	−0.415	−0.468
		750↑	0.175	−0.226
		761↓*	0.723	0.798
		770↑	0.136	0.031
			0.023	0.012
			0.089	0.049
			0.189	0.124
			0.352	0.262
			0.466	0.392
			0.440	0.499
			0.328	0.456
		770↑*	0.561	0.550

almost always much larger than any of the rest, indicating an almost pure state. The eigenvector with this coefficient can appropriately be termed the dominant eigenvector of the set, and, since the role of $\chi_\Omega{}^N$ is governed mainly by this dominant eigenvector, it is not unreasonable to allow it to characterize the state $\chi_\Omega{}^N$. Thus we obtain $\chi_\Omega{}^{NN_z}$. Comparison of the coefficients A_{NN_z} can readily be made from Table II.

The eigenvalues r are obtained from an exact diagonalization of the dimensionless matrices containing elements of $(H'/\hbar\omega_0)-\frac{1}{3}(3N_z-N)\epsilon$ for given N and Ω. The term in ϵ is diagonal in N and N_z. As mentioned previously, the choice of C and D is the same as in Nilsson's paper.

The level spectrum from $N=4$ through $N=7$ was obtained, with diagonalization of matrices larger than

3×3 being done on the digital computing SWAC at the University of California at Los Angeles. The largest matrix was 8×8. The region of deformation was restricted to positive values of ϵ, specifically 0.2 and 0.3. The results are placed in Table II which will be explained shortly.

B. Arrangement of Tables and Diagrams

In Table II we present the coefficients A_{NN_z} of the normalized wave functions $\chi_\Omega^{NN_z}$ for the neutron spectrum from $N=4$ through $N=6$ and those few for $N=7$ which lie low enough to be included in the spectrum. The A_{NN_z} values are given for the cases $\epsilon=0.2$ and 0.3. Because of limitations of space, the coefficients A_{NN_z} of the proton spectrum have not been given here except for the case $N=5$, $\Omega=\frac{1}{2}$,[9] which has been given for both proton and neutron spectra in Table III to illustrate the quantitative similarity between neutron and proton wave functions of the same set of quantum numbers and deformation value. In most instances the neutron wave functions are adequate for computational purposes involving either protons or neutrons.

A particular set of coefficients can be identified through the eigenvector in the extreme left-hand column, once a particular N, Ω, and ϵ have been selected. These eigenvectors are the dominant eigenvectors previously mentioned. The vertical order in which these dominant eigenvectors appear is the order of the base vectors for the expansion of $\chi_\Omega^{NN_z}$. Immediately adjacent to the dominant eigenvector we have included the orbit numbers prescribed by Nilsson. In some instances these numbers are missing. This occurs whenever the level in question lies outside the range of Nilsson's[4] energy level diagram (his Fig. 5). To obtain a $\chi_\Omega^{NN_z}$, let us consider, as an example, the case of $N=6$, $\Omega=\frac{5}{2}$, and $\epsilon=0.2$. Keeping the base vectors for the expansion coefficients in the vertical sequence, we can obtain the corresponding expansion coefficient by reading them off in a similar order. To illustrate further, let us choose orbit number 72. The resulting total wave function is

$$\chi_{\frac{5}{2}}^{62}=0.215\langle 602\uparrow\rangle+0.170\langle 613\downarrow\rangle+0.806\langle 622\uparrow\rangle -0.485\langle 633\downarrow\rangle-0.200\langle 642\uparrow\rangle. \quad (9)$$

The dominance of $\langle 622\uparrow\rangle$ is immediately apparent.

III. APPLICATION OF RESULTS

A. Presentation of Energy Levels

Following the scheme of classifying nucleonic states used by Mottelson and Nilsson,[10] we present separate level spectra for neutrons and protons. This separation results from a different choice of D values such that higher angular momentum states are pulled down for the proton to get better agreement with experimental results (see reference 10). In Fig. 1(a) we give neutron levels corresponding to a D value of $-0.0225\hbar\omega_0$ and $C=-0.1\hbar\omega_0$. The levels correspond to the eigenvalues E_{NN_z} given by Eq. (8) as functions of the deformation parameter ϵ. Each level is given by a straight line through two values of E_{NN_z} calculated for $\epsilon=0.2$ and 0.3. The line is then extrapolated to $\epsilon=0.15$ on the smaller-deformation side and to $\epsilon=0.35$ in the strong-deformation region. The extension of these lines was made to clarify the presentation of the level spectra. A comparison with the more exact curves can be made via Nilsson's Fig. 5. From this comparison it will be observed that in the region of interest, $\epsilon=0.2$ to 0.3, one does not commit too serious an error in approximating these curves by straight lines, especially since the level ordering is not to be taken too literally when they are several close-lying states (e.g., pairing energy corrections need to be taken into account when considering actual level ordering). In the main, the level

TABLE III. Comparison of the neutron and proton-eigenfunctions for $N=5$, $\Omega=\frac{1}{2}$. (See caption of Table II.)

				Neutrons		Protons	
N	Ω	ψ		$\epsilon=0.2$	$\epsilon=0.3$	$\epsilon=0.2$	$\epsilon=0.3$
5	$\frac{1}{2}$	501↓	A	0.955	0.970	0.952	0.968
				−0.224	−0.190	−0.203	−0.175
				−0.177	−0.142	−0.208	−0.169
				0.078	0.050	0.082	0.054
				0.027	0.017	0.040	0.025
				−0.017	−0.008	−0.022	−0.010
				0.155	0.146	0.142	0.132
		510↑	71	0.874	0.916	0.872	0.914
				−0.357	−0.295	−0.306	−0.263
				−0.250	−0.207	−0.317	−0.259
				0.147	0.089	0.148	0.095
				0.033	0.023	0.067	0.041
				0.227	0.181	0.238	0.197
				0.163	0.166	0.097	0.122
		521↓	63	0.738	0.834	0.723	0.823
				−0.476	−0.409	−0.431	−0.384
				−0.288	−0.234	−0.363	−0.298
				0.260	0.147	0.307	0.180
				0.062	0.051	0.086	0.057
				0.333	0.279	0.394	0.318
				0.105	0.185	0.189	0.183
		530↑	53	0.647	0.756	0.614	0.742
				−0.665	−0.533	−0.522	−0.468
				−0.116	−0.171	−0.390	−0.304
				0.084	0.045	0.080	0.050
				0.156	0.096	0.043	0.061
				0.435	0.341	0.435	0.358
				0.102	0.156	−0.165	0.002
		541↓	47	0.391	0.615	0.532	0.633
				−0.785	−0.685	−0.701	−0.682
				0.045	0.024	0.055	0.032
				0.156	0.095	0.181	0.120
				0.311	0.215	0.341	0.251
				0.526	0.437	0.551	0.481
				0.547	0.524	0.537	0.531
		550↑	38	0.549	0.692	0.507	0.639

[9] Tables of the A_{NN_z} for protons are available upon request from the Physics Department, University of California at Los Angeles, Los Angeles, California.

[10] B. R. Mottelson and S. G. Nilsson, Phys. Rev. **99**, 1615 (1955). It should be noted that several states with large negative slopes are missing from the neutron spectrum of this reference. Some of these come from the $N=7$ shell.

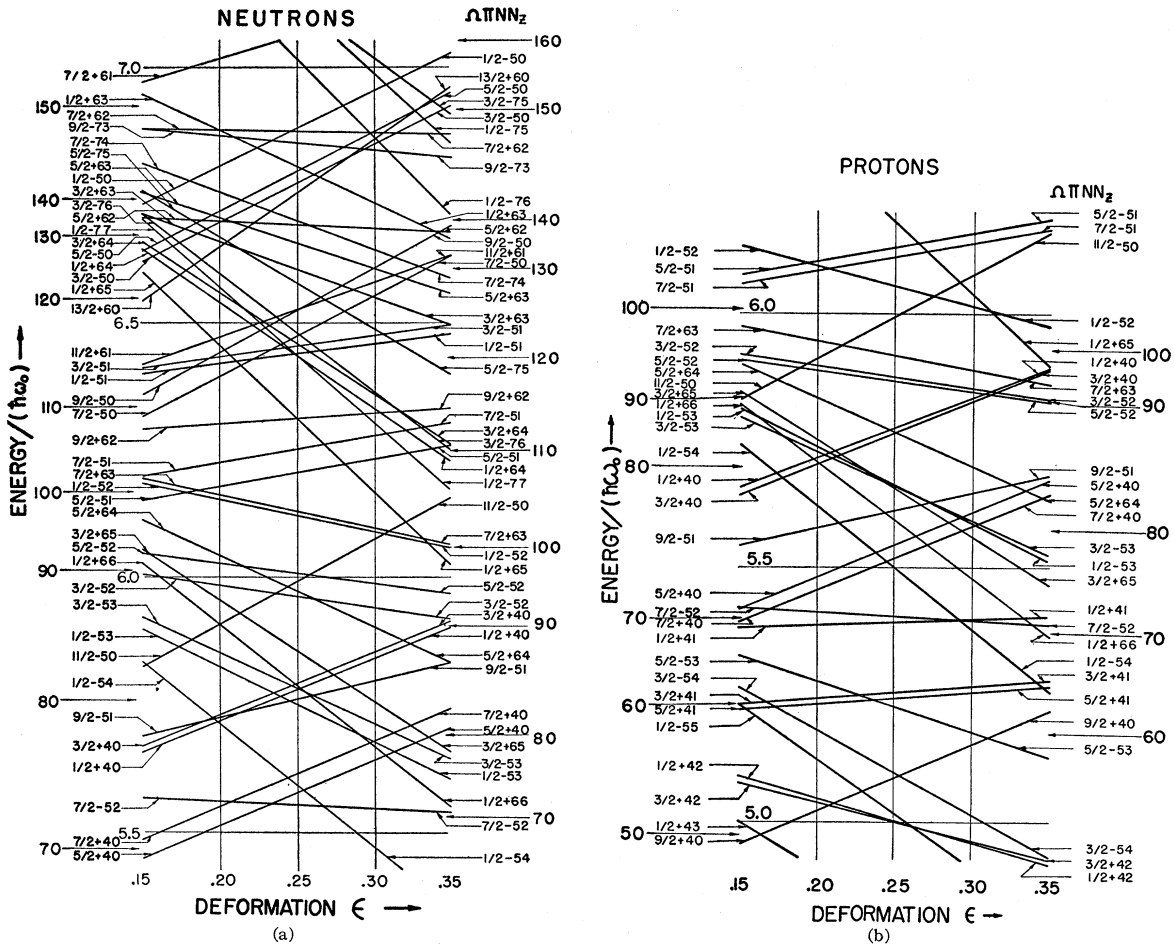

FIG. 1. (a) Level spectrum for neutrons $70<N<160$ in a deformed field given by Eqs. (1a) and (1b) with strong positive deformation and values of $C=-0.1\hbar\omega_0$ and $D=-0.0225\hbar\omega_0$. Since the energy in the strong-deformation region ($\epsilon>0.2$) is generally a monotonic function with not too great a curvature. the true curves have been approximated by straight lines through two values of the energy for $\epsilon=0.2$ and 0.3, respectively. The levels are marked off in groups of five on either side of the figure to facilitate locating them. Each level is labeled by spin, parity, and asymptotic quantum numbers N and N_z in that order. (b) Level spectrum for protons $50<Z<100$ similar to Fig. 1(a), except for D. Here $D=-0.0275\hbar\omega_0$.

ordering in the above-stated region follows the exact (Nilsson) ordering sufficiently well to allow a classification of nucleonic states, which is all it has been intended to do.

A convenient system for locating the levels by particle number has been given to facilitate the sometimes frustrating job of locating levels. The levels are separated off in groups of five (recall that each line is two-fold degenerate corresponding to $\pm\Omega$ values) by extended lines on either side of the level scheme. Each level is identified through values of Ω, parity, and the asymptotic quantum numbers N and N_z in that order. The entire level scheme is placed on a grid pattern where the vertical lines mark off the regions of deformation in steps of $\epsilon=0.05$, while the horizontal lines give the energy. As in Nilsson's Fig. 5, the energy scale is to $(E/\hbar\omega_0)(1+\epsilon^2/9)$. Also, the true energy scale varies with A, since as Nilsson points out, $\hbar\omega_0$ may be assumed to depend on A as $A^{-1/3}$ (Nilsson, p. 18). The range of the neutron spectrum is for neutron numbers 70 to 160.

The proton level scheme, Fig. 1(b) is similar in construction to the neutron scheme, there being two differences. First a D value of $-0.0275\hbar\omega_0$ is chosen, thereby favoring the states of higher l-values, and secondly the plot is for protons numbers 50 to 100.

An interesting feature of the neutron spectra is the large gap at $N=152$ in the range of ϵ near 0.2, which seems to indicate shell structure at that region. Evidence for a subshell at $N=152$ has been previously reported by Ghiorso *et al.*,[11] in connection with discontinuities in alpha-decay energies near 152 neutrons. It has been pointed out by them that this subshell may be of a fundamentally different nature than the major closed shells since, on the basis of the strong-coupling model, the first-excited-state energies should approach

[11] Ghiorso, Thompson, Higgins, Harvey, and Seaborg, Phys. Rev. **95**, 293 (1954).

a maximum for configurations involving only completely filled levels; a trend which so far has not been substantially supported by experimental evidence. For example, in a plot of energies of first excited states of heavy even-even nuclei by Hollander,[12] the rate at which the energies of the first excited states in curium rise as $N=152$ is approached turns out to be less than that of nearby neighbors, uranium and plutonium, of lesser neutron number. It should be pointed out in connection with this, however, that it is generally characteristic of strongly deformed nuclei to possess rather low-lying rotational states as first excited states. These low-lying rotational states are generated from the ground state configuration and, therefore, there need not be any low-lying particle transition levels for nuclei for $N=152$. In fact this is just what is implied by the spectrum gap at $N=152$. Hence, except for low-lying rotational levels, the subshell should be of the same nature as the major closed shells. An indication in this direction is given by the sequence of levels, where it is seen that the last of the $N=5$ shell levels is filled at the gap.

B. Selection Rules

As suggested by Nilsson (reference 4, Appendix B), the introduction of the new quantum numbers N_r and Σ should have associated with them new selection rules for particle transitions. In Alaga's paper,[8] a general classification of allowed and first-forbidden β transition selection rules has been given for transitions between the unperturbed states of the asymptotic representation within a given rotational group; i.e., he excludes rotational branching and $\mathbf{K}$[13] forbidden transitions. We shall here give approximate selection rules for particle transitions between the states $\chi_\Omega^{NN_z}$ of the total single-particle Hamiltonian.

Following Alaga, we call those transitions which are permitted by all the selection rules unhindered; those transitions which are allowed by $\Delta\Omega$ and I but forbidden by any of the remaining selection rules we call hindered. We shall give special attention to the hindered transitions to further classify them according to speeds allowed by selection rules for particle transitions between the $\chi_\Omega^{NN_z}$'s.

[12] J. M. Hollander, Phys. Rev. **103**, 1591 (1956).

[13] $\mathbf{K}$ is defined as the projection of the nuclear spin I on the nuclear symmetry axis.

TABLE IV. Approximate selection rules for first forbidden transitions: Asymptotic representation.[a]

$\Delta\Omega$ \ ΔN_r	Fast	Slow $10^{-3}-10^{-1}$	Very slow $10^{-5}-10^{-3}$
1	1	...	≤ 0 or ≥ 2
0	0	1 or 2	≤ -1 or ≥ 3
-1	1	-1 or 0	≤ -2 or ≥ 2

[a] For $\Delta N=-1$, the signs are everywhere reversed.

An examination of the $\chi_\Omega^{NN_z}$'s in expanded form reveals that although they are almost pure in many cases, the admixture of the unperturbed $\psi_{NN_z\Omega}$'s is sufficient to significantly alter the transition matrix element values. In fact, in some transitions these impurities at times are capable of giving rise to matrix elements which are of the order of one tenth of the unhindered elements.

To illustrate let us consider allowed β transitions. For each selection rule $\Delta\Omega=\pm 1$ or 0, a semiquantitative measure of the relative speeds of the transitions can be obtained from the following relation: For a given $\Delta\Omega$,

$$|\int\sigma|^2_{\Delta N_z}/|\int\sigma|^2_{\Delta N_z'}\sim 10^{-|\Delta N_z|+|\Delta N_z'|}, \qquad (10)$$

for all ΔN_z except zero. When ΔN_z does equal zero, two cases arise, namely, (1) if $\Delta\Sigma=\Delta\Omega$ or zero we get the fast or unhindered transitions, and (2) for $\Delta\Sigma=-\Delta\Omega$ except zero, we get a relative speed of 10^{-1}.

Similarly, for first-forbidden β transitions we have the classification for $\Delta N=1$ given in Table IV. The selection rules of Table IV apply also to $E1$ transitions, where generally the low-energy $E1$ speeds are in the "very slow" class. These selection rules are based on exact calculations of a representative number of transition matrices. The elements were compared and classified as explained above.

ACKNOWLEDGMENTS

I would like to express my appreciation for the contributions to this work of Dr. Steven A. Moszkowski, who suggested the problem and whose guidance and advice stimulated its progress.

I would also like to thank Dr. Michel Melkanoff for his help in diagonalizing the matrices on the SWAC at the University of California at Los Angeles.